CHAPTER V

ANALYSES OF SLOPE STABILITY

5.1 Factors Affecting Slope Stability Analyses

5.1.1 Geomechanics classification for intact rocks

A classification for the rock material strength, compared to the previous works, has been proposed by Bieniawski (1973) (Table 12). It is thus clear from the unconfined compressive strength test results of claystones in the previous chapter that they indicate a very low strength property, i.e., the claystones behave like rock as well as soil. Therefore, the methods of analysis used in this chapter have both soil and rock mechanics approaches.

5.1.2 Slope height and slope angle

For the maximum slope height and slope angle relationship for cut slopes, Hoek and Bray (1974) stated that even if one accepts that the stability of a rock mass is dominated by geological discontinuities, there must be situations where the orientation and inclination of these discontinuities is such that simple sliding of slabs, blocks or wedges is impossible. Failure in these slopes will involve a combination of movement on discontinuities and failure of intact rock material and one would anticipate that in such cases, higher and steeper slopes than average could be excavated.

Table 12. Classification for strength of intact rock. (after Bieniawski, 1973).

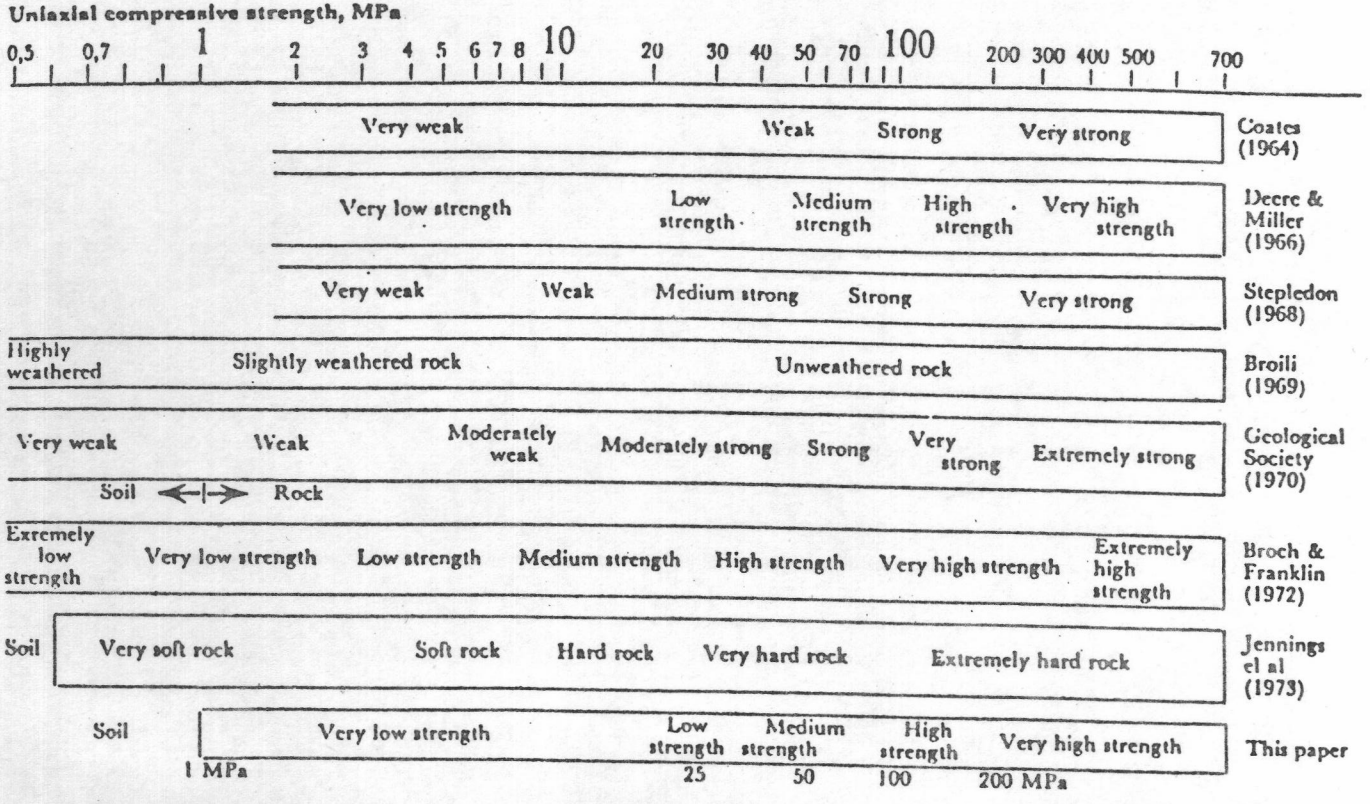

In order to determine the maximum height (H_{max}), Terzaghi (1963) derived equation for the height of vertical part of the slope as :

$$H_{max} \leq \frac{c}{\gamma \cos \alpha (\sin \alpha - \cos \alpha \tan \phi)}$$

where c = cohesion

ϕ = internal friction angle

γ = bulk density

α = slope angle

To determine the maximum height of intact rock materials forming a slope in the study area, intact shear strength parameters (for C_p-peak cohesion and ϕ_p-peak internal friction angle) of claystones from Table 6 and the bulk density were substituted in the equation above for an overall slope angle of, say, 30°. It shows that the slope height can be as high as 157 meters or more without any failure occurred. Therefore the main factors that determine the slope stability are not the peak cohesion, but the residual shear strength parameters, namely residual cohesion (C_r) and residual friction angle (ϕ_r); the values are obtained from the defect shear strength test.

5.1.3 Water condition

Rain water which penetrates the ground as groundwater affects the shear strength of any two intact surfaces in two ways. If the hydraulic gradient is high, the water pressure between the two surfaces may build up and effectively reduce the shear strength along the two surfaces. In the case of Mae Moh lignite mine, even though the permeability of intact claystones forming a slope is very low, the high water pressure

built up may be possible because these rocks together with a few porous lignite beds are extensively jointed. A large amount of water may fill these discontinuities during the wet season, hence create a high water - pressure condition. The other effect from the penetrating is groundwater that the water acts as a lubricant on these surfaces, thus the friction against the displacement of the two blocks passing each other is reduced.

Groundwater table is also important for the evaluation of pore water pressure in the stability calculation. Unfortunately the resistivity determination for groundwater table in this work is still incomplete because the resistivity contrast between the unsaturated and saturated zones in the claystones is very low as mentioned in Chapter III. It is hence necessarily to assume a reasonable groundwater condition for the stability calculation. The assumption was based on the fact that during the wet season, heavy rain fall occurs and the materials composing slope can thus be partially to fully saturated with rain water depending on the quantity of rain water and properties of slope materials. The partially and fully saturated conditions for slope stability calculation were set out according to the appropriate assumption of the method of analysis to be mentioned later.

5.1.4 Planes of weakness

The presence or absence of discontinuities in rock slope has a very important influence on the stability of rock slopes. Any failure will tend to be controlled by these planes of weakness. Three types of planes of weakness in the study area were mapped and studied in detail.

The study result is reported in Plate I. These planes of weakness are as follows.

5.1.4.1 Bedding planes

It is important to note that the orientation of the slope with respect to that of the bedding plane has a major effect on the stability. Slopes where the bedding plane dips away from the pit tend to be more stable than slopes where the bedding plane dips into the excavated area. The slope in Subareas 1, 2, 3, and 4 are considered to be more stable than that in Subarea 5 where the bedding plane dips into the excavated area. Thus planar-bedding plane sliding is expected to be occurred in Subarea 5.

5.1.4.2 Joint planes

The pervasive joint sets in the study area are steeply to vertically dipping tension joints. These joints help create the slope failure in various means. They are as follows.

a) If the strike of joints is parallel or sub-parallel to the slope face, they can cause the toppling failure.

b) If the intersection line of the two joint planes emerges on the slope face, they can cause wedge failure.

c) If the intersection line of a joint with other discontinuity, e.g. fault, emerges on the slope face. They also can cause wedge failure.

d) Rain water can seep as groundwater into the slope mass by passing through these joints, thus cause instability of slope-as mentioned in section 5.1.3.

5.1.4.3 Fault planes

In the study area only a few major faults were found. The strike of these faults cuts across the slope, especially in Subareas 3 and 4. Similar to the joints, these faults may cause the slope failure at some specific locations when :-

a) the intersection line of fault and joint emerges on the slope face, the condition is found in Subarea 3, or

b) the intersection line of the two faults emerges on the slope face, this condition is found in Subarea 4.

As the claystones also behave like soil meterials, another possible plane of weakness can occur in the form of an arc of circle. In the study area, slope material is stratified and jointed and the shearing strength of individual strata is approximately the same, the failure path can pass through the combination of those discontinuities in slope mass. For this reason, the slip surface will be a slightly hackly curve that, if the jags are neglected, can be considered as an approximate arc of circle.

5.1.5 Seismological effects

The results of seimic activity can have a negative on slope stability. In slopes at or near limiting equilibrium, the lateral

accelerations due to a seismic event may be sufficient to initiate failure to the pit slope.

Longworth-CMPS (1981) reported no local major seismic event though the regional data indicate that northern Thailand is not completely seismic-free. To date, no earthquake has ever been recorded in the Mae Moh basin, thus the seismological effect is precluded for the stability analysis in this work.

5.1.6 Factor of safety

Factor of safety for the slope failure is defined as the ratio of the total force available to resist sliding to the total force tending to induce sliding. At the point of failure, a condition of limiting equilibrium exists in which the resisting and driving forces are equal and then the factor of safety (F.S.) = 1. When the slope is stable, the resisting forces are greater than the driving forces and the factor of safety is larger than unity.

Hoek and Bray (1974) suggusted from their practical experience that an increase in the factor of safety from 1.0 to 1.3 will generally be adequate for mine slopes which are not required to remain stable for a long period of time. For the critical slopes adjacent to haul roads or important installations, a factor of safety of 1.5 is more preferred. The significance of the safety factor for soil masses given by Sowers (1979), shown as Table 13 below, gives a similar significance to Hoek and Bray's suggestion.

Table 13. Significance of safety factors for design (after Sowers, 1979).

Safety factor	significance
1.0	Unsafe
1.0-1.2	Questionable safety
1.3-1.4	Satisfactory for cuts, fills, questionable for dams
1.5-1.75	Safe for dams

In the study area, the stability of the northwestern flank slopes would receive a serious consideration since they locate near to the existing power plants and haul roads. Therefore, the factor of safety of 1.5 is used as a guide line for the stability assessment here. For the other slopes, the factor of safety of 1.0 to 1.3 is used instead.

5.2 Method of Slope Stability Analyses

The analysis for slope stability of each subarea of study was done by selecting the proper methods shown in Table 14. These methods are all the limiting equilibrium kinds. The basic assumption of a limit equilibrium approach is on Coulomb's failure criterion which must be satisfied on the assumed failure surface, no matter whether the surface be a straight line, circular arc or other irregular surface.

In the present study, all three types of possible slope failure, plane failure, wedge failure, and circular failure were calculated for

Table 14. Methods of analysis used for each subarea of study.

Subarea	Observed stability condition	Possible failure types	Method of analysis
1	Stable.	Circular arc.	2, 3
2	Unstable; local slump, small scale wedge failure.	Circular arc, wedge.	1, 2, 3
3	Unstable; wedge failure, landslide, vertical slab failure.	Circular arc, wedge, vertical slab failure.	1, 2, 3
4	Unstable; rock fall, possible wedge failure.	Circular arc, wedge.	2, 3
5	Unstable; planar sliding.	Bedding plane failure.	1, 4

Notations :- 1 = Stereographical method

2 = Hoek and Bray stability charts method

3 = Simplified Bishop method of slices

4 = Plane failure analysis

the factor of safety because their failure processes involve a simple gravitational sliding. If the failure process does not involve a simple gravitational sliding, e.g. in the case of toppling failure, the factor of safety can not be calculated for. This is fortunately not a case in this area.

The methods of stability analysis which are mentioned in Table 14 are reviewed as follows.

5.2.1 Stereographical method

Hoek and Bray (1974) had simplified from Markland (1972) four main types of failure diagrams as show in Figure 33. The figure illustrates the typical stereographical plots of geological conditions likely lead to slope failures.

The graphical method for stability analysis used in this work, however, consists of two techniques. One is Markland's technique (1972) as mentioned in Hoek and Bray (1974), and the other is the technique developed by Hendron et al. (1971). Both techniques are further described below.

The Markland's technique is used to evaluate the possibility of failure. By drawing the great circle representing slope face, the friction circle and the great circle representing discontinuities planes in an equal-area stereographic projection, one can recognize the discontinuity planes which represent the potential failure planes, and can eliminate those which are unlikely to be involved in slope failures.

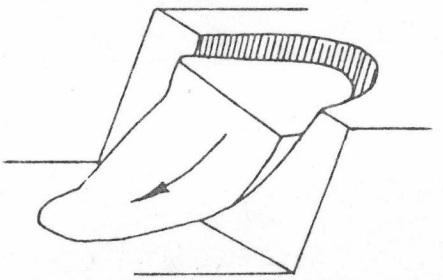

a. Circular failure in overburden soil, waste rock or heavily fractured rock with no identifiable structural pattern.

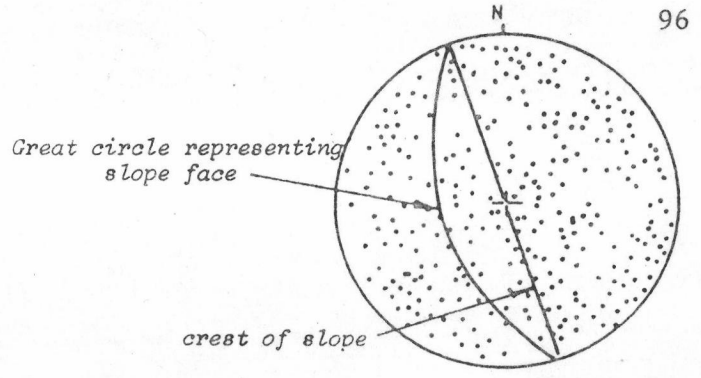

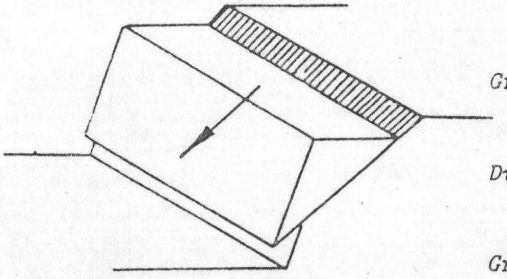

b. Plane failure in rock with highly ordered structure such as slate.

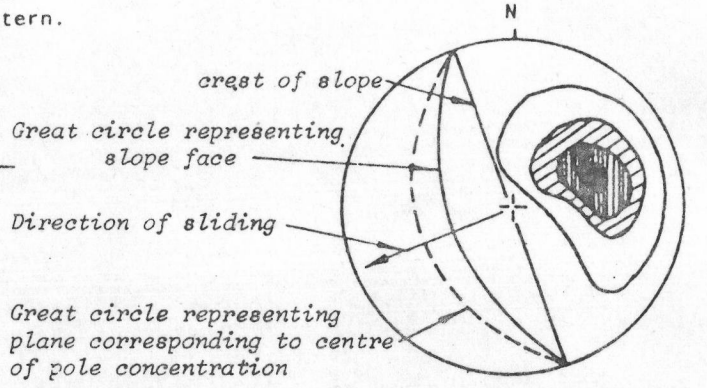

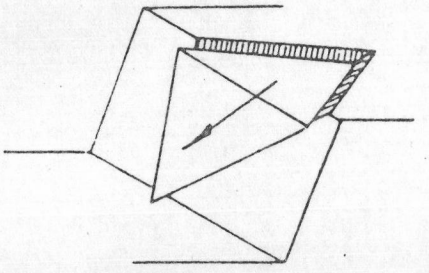

c. Wedge failure on two intersecting discontinuities.

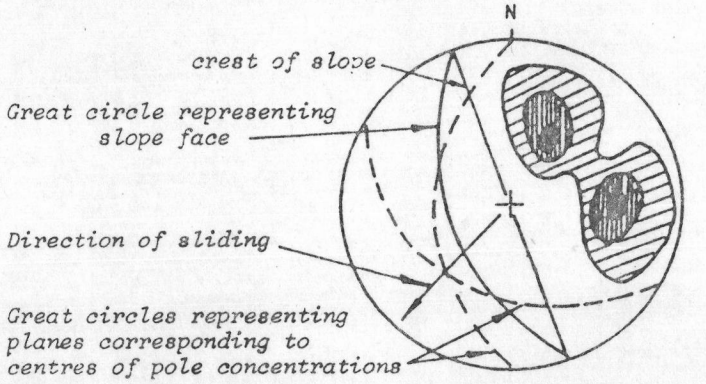

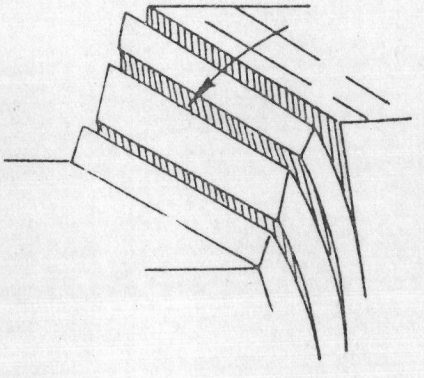

d. Toppling failure in hard rock which can form columnar structure separated by steeply dipping discontinuities.

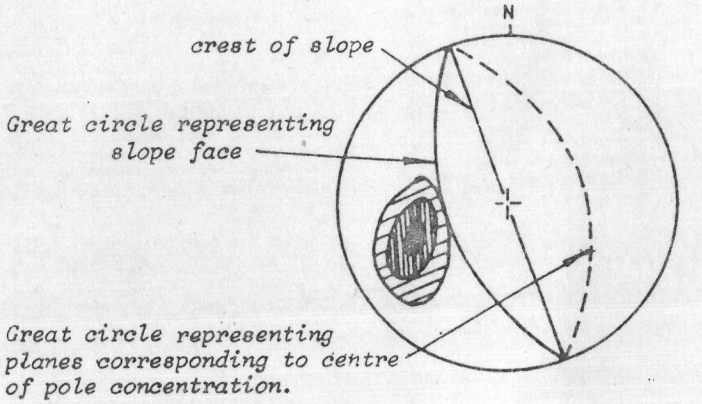

Figure 33. Main types of slope failure and appearance of stereoplots of conditions likely to give rise to these failures. (after Hoek and Bray, 1974).

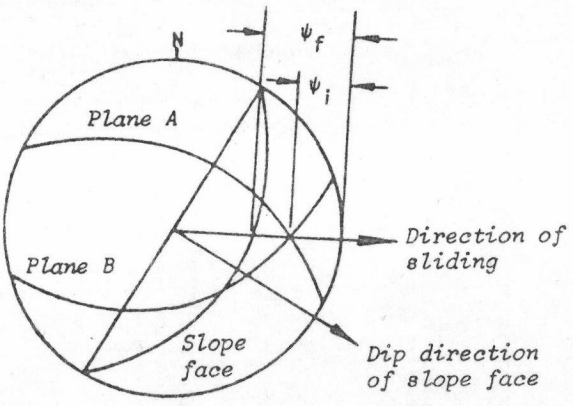

a: Sliding along the line of intersection of planes A and B is possible when the plunge of this line is less than the dip of the slope face, measured in the direction of sliding, ie

$$\psi_f > \psi_i$$

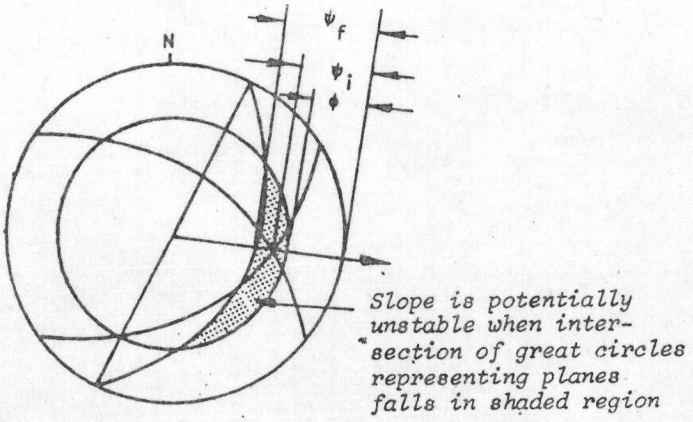

b : Sliding is assumed to occur when the plunge of the line of intersection exceeds the angle of friction, ie

$$\psi_f > \psi_i > \phi$$

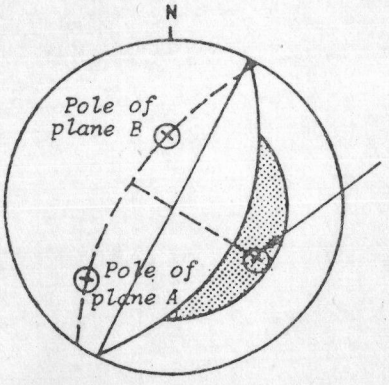

c : Representation of planes by their poles and determination of the line of intersection of the planes by the pole of the great circle which passes through their poles.

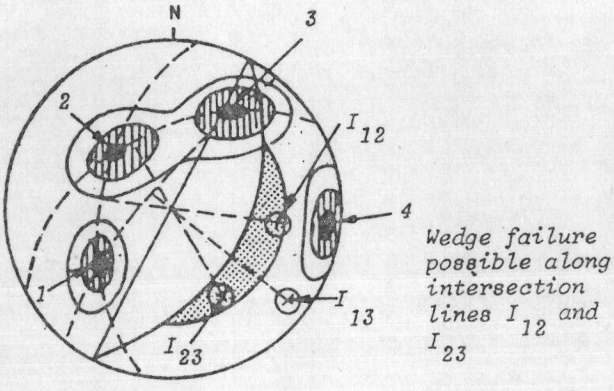

d : Preliminary evaluation of the stability of a 50° slope in a rock mass with 4 sets of structural discontinuities.

Figure 34. An example of Markland's technique for wedge failure analysis. (after Hoek and Bray, 1974).

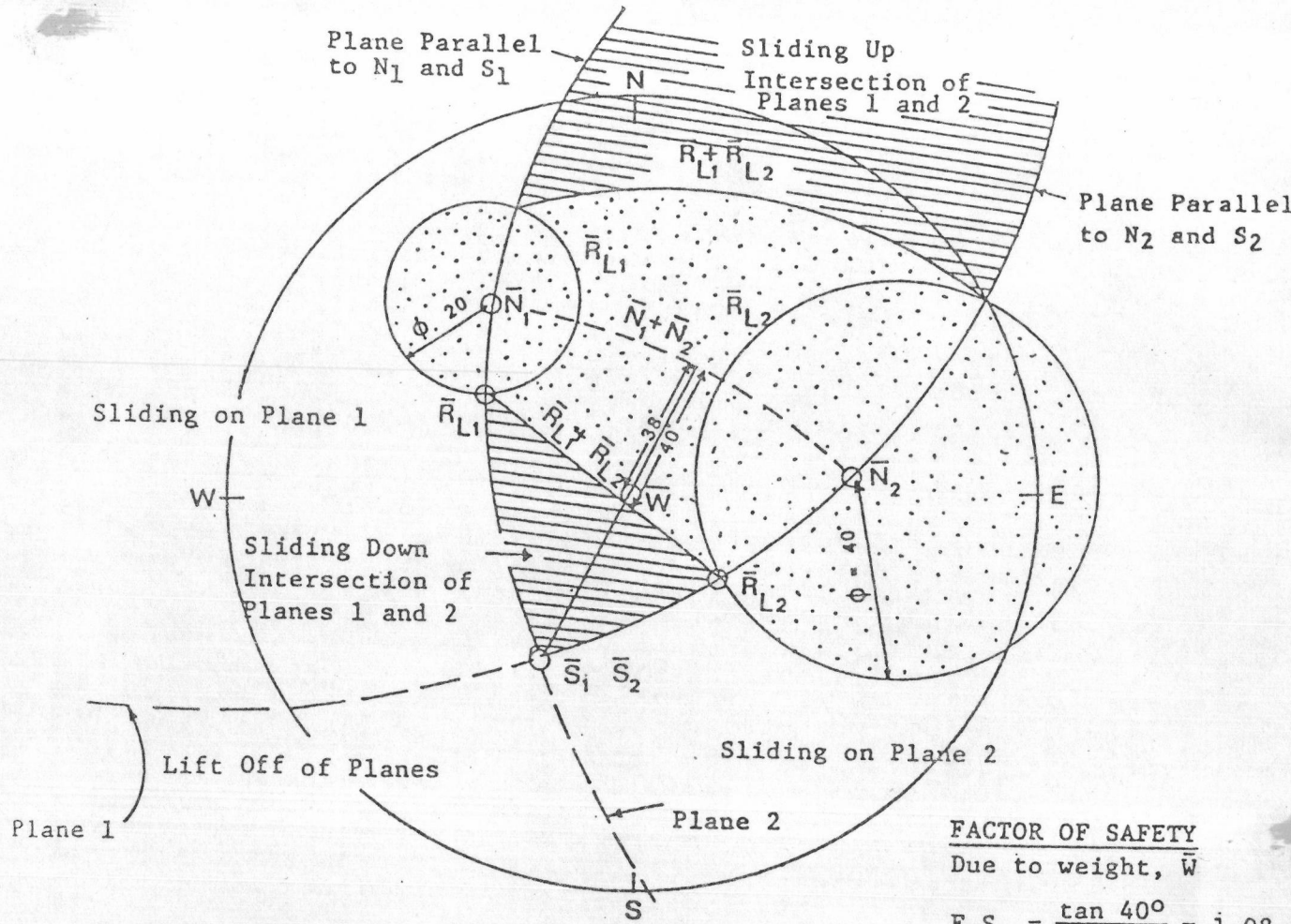

FACTOR OF SAFETY

Due to weight, $\bar{W}$

$$F.S. = \frac{\tan 40^o}{\tan 38^o} = 1.08$$

$\bar{N}_1$, $\bar{N}_2$ are normal forces of plane 1 and plane 2 located at the poles of planes

$\bar{S}_1$, $\bar{S}_2$ are maximum shear forces of plane 1 and plane 2, plot on the stereogram at the same point as does the line of intersection of plane 1 and plane 2

$\bar{R}_{L1}$, $\bar{R}_{L2}$ are reaction forces at failure (summation of the normal forces $\bar{N}_1$, $\bar{N}_2$ and maximum shear forces $\bar{S}_1$, $\bar{S}_2$), $\bar{R}_{L1}$ located where a great circle through $\bar{N}_1$ and $\bar{S}_1$ intersects the friction cone of plane 1.

$\bar{N}_1+\bar{N}_2$ is a great circle of $\bar{N}_1$, $\bar{N}_2$

$\bar{S}_1+\bar{S}_2$ is a great circle of $\bar{S}_1$, $\bar{S}_2$

Figure 35. An example of Hendron et al.'s technique for wedge failure analysis.

An example of Markland's technique is shown in Figure 34.

The technique of Hendron et al. (1971) used for finding the factor of safety is done by plotting the poles of discontinuity planes which involve the slope failure, and the cone of friction angle around them on an equal-angle stereonet. The plot thus illustrates the zone of stable area and the resultant resisting force ($R_{L1} + R_{L2}$ in Figure 35). The resultant driving force (W) thus gives the factor of safety. An example of this technique is also shown in Figure 35.

5.2.2 Hoek and Bray stability charts method

Hoek and Bray (1974) developed the circular failure charts for slope stability calculation. Their charts illustrated in Figure 37 (a) to (e) were plotted by a Hewlett-Packard 9100B microcomputer with graph plotting facilities. In this method, the failure surface is assumed to cut through the toe of the slope. The graphic solution is done on cases of different groundwater condition. Five cases are considered (Figure 36), each case with a different chart (Figure 37 (a) to (e)). The steps of consideration are as follows.

5.2.2.1 Decide on which groundwater condition is applicable.

5.2.2.2 Calculate the value of $\frac{C}{\gamma H \tan \phi}$

where; H = Height of slope,

γ = Bulk density of slope material

C = Cohesion

ϕ = Friction angle.

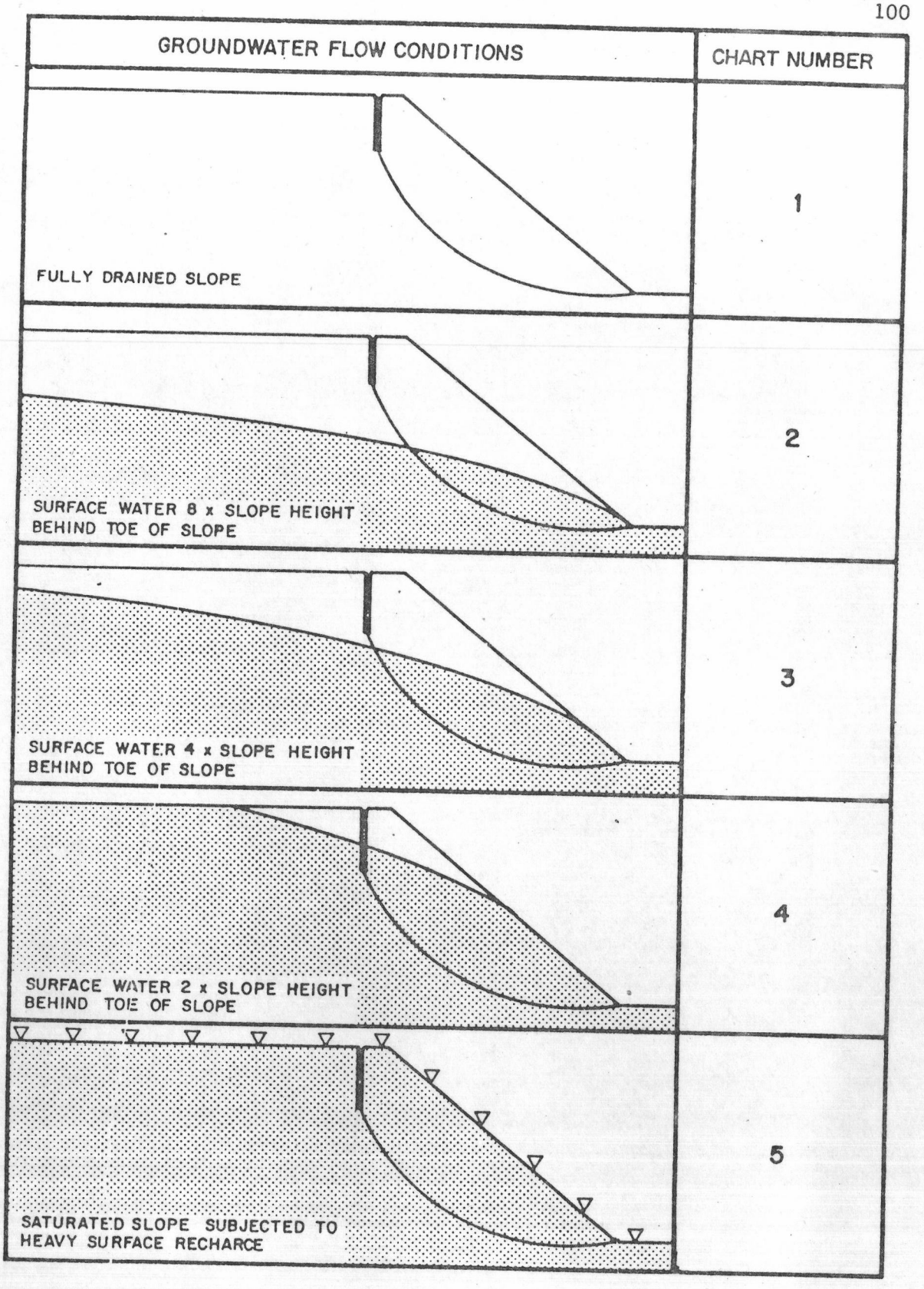

Figure 36. Groundwater conditions for various charts. Chart numbers 1 to 5 are shown in Figure 37 a to e respectively (after Hoek and Bray, 1974).

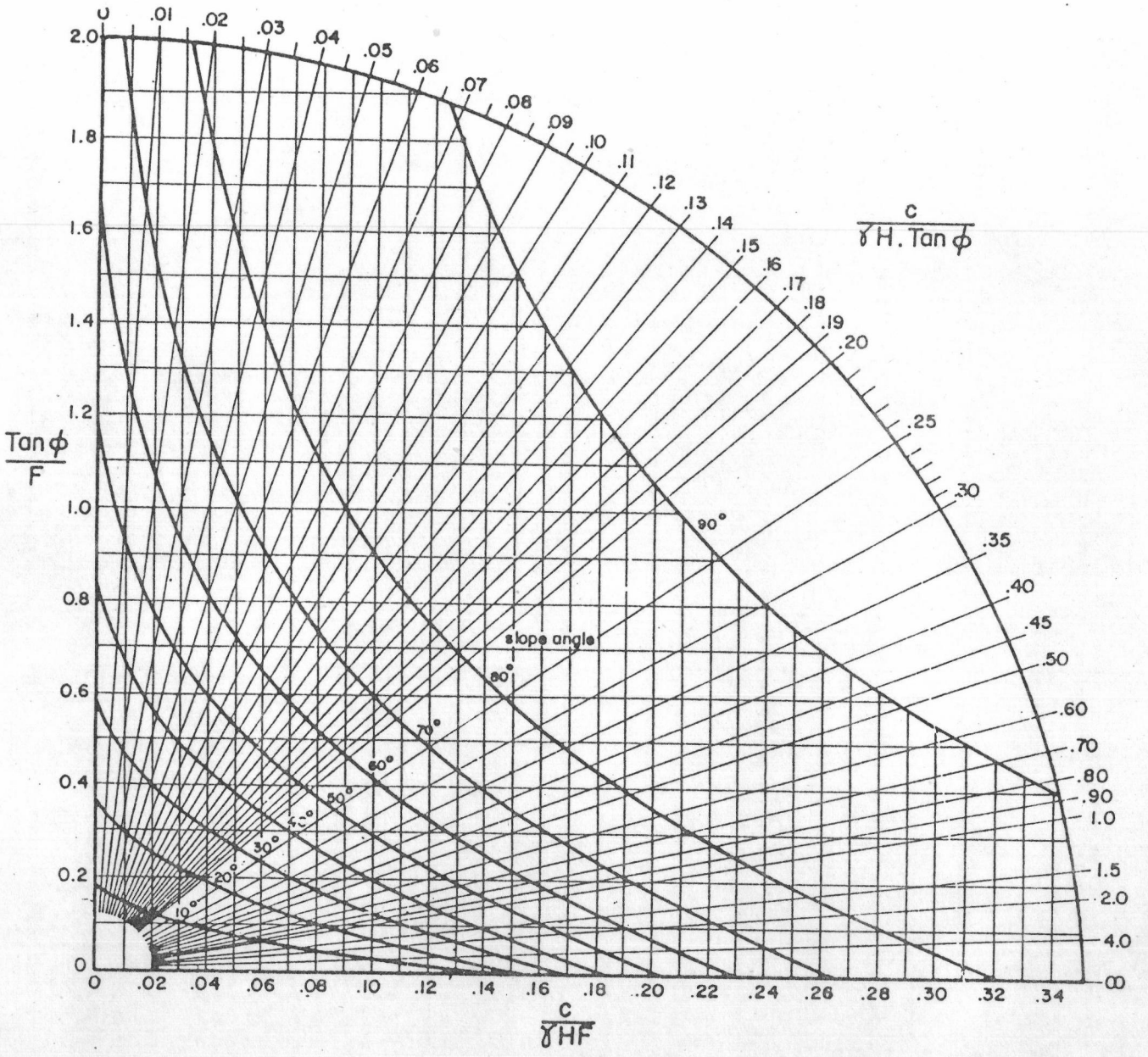

Figure 37. Circular failure chart number 1 to 5 of Hoek and Bray (1974).

(a) Circular failure chart number 1.

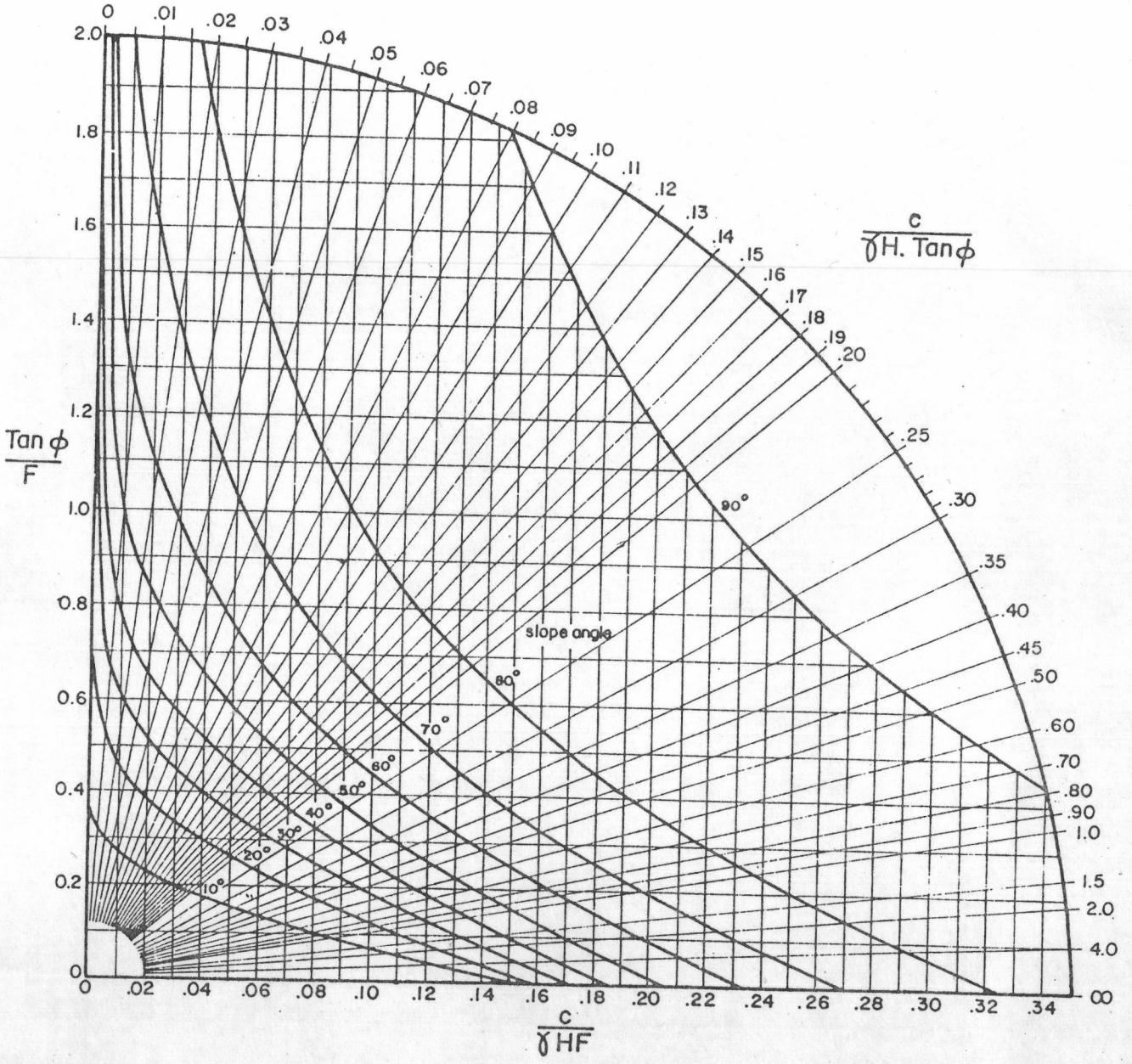

Figure 37. cont.

(b) Circular failure chart number 2.

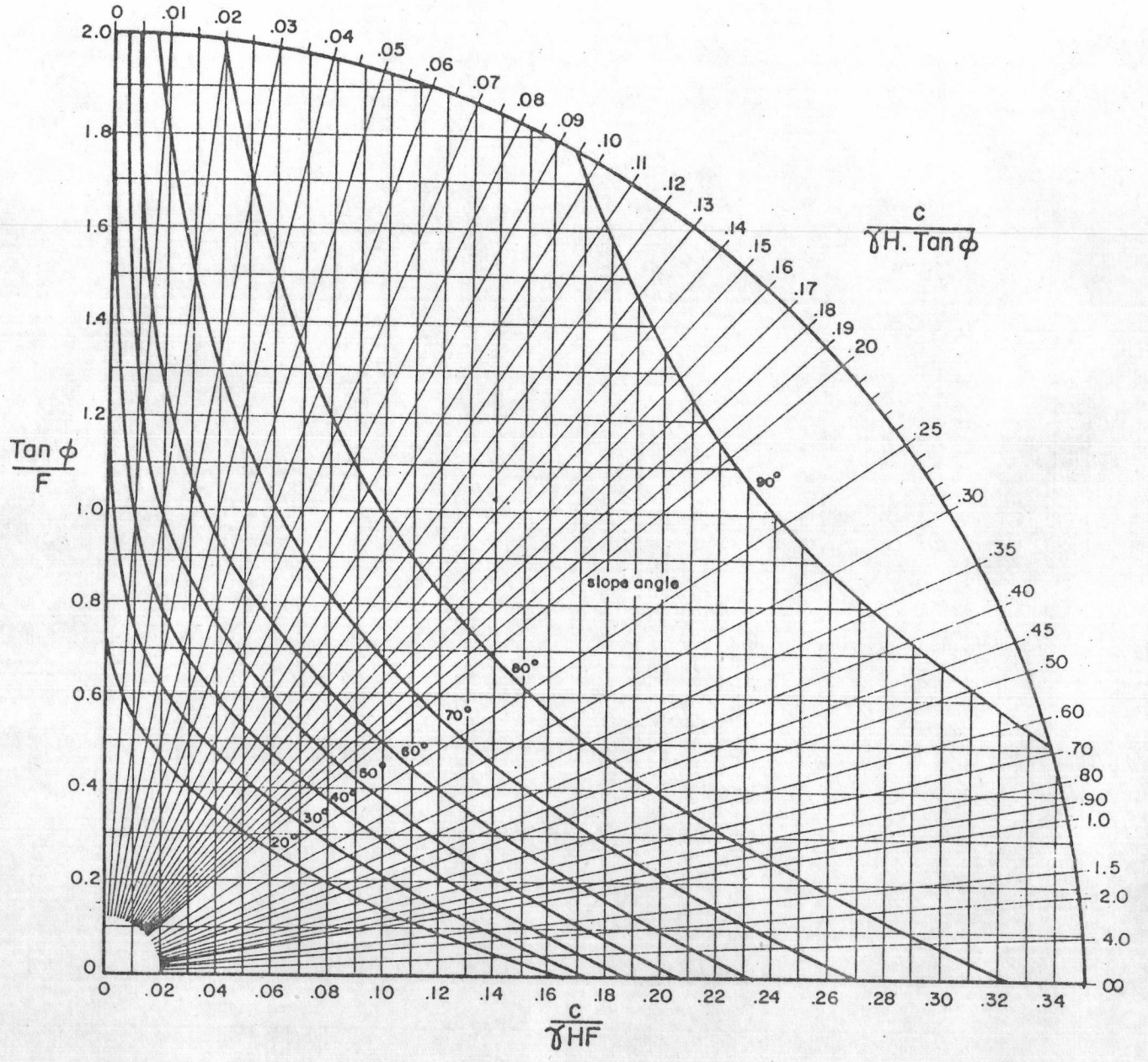

Figure 37. cont.

(c) Circular failure chart number 3.

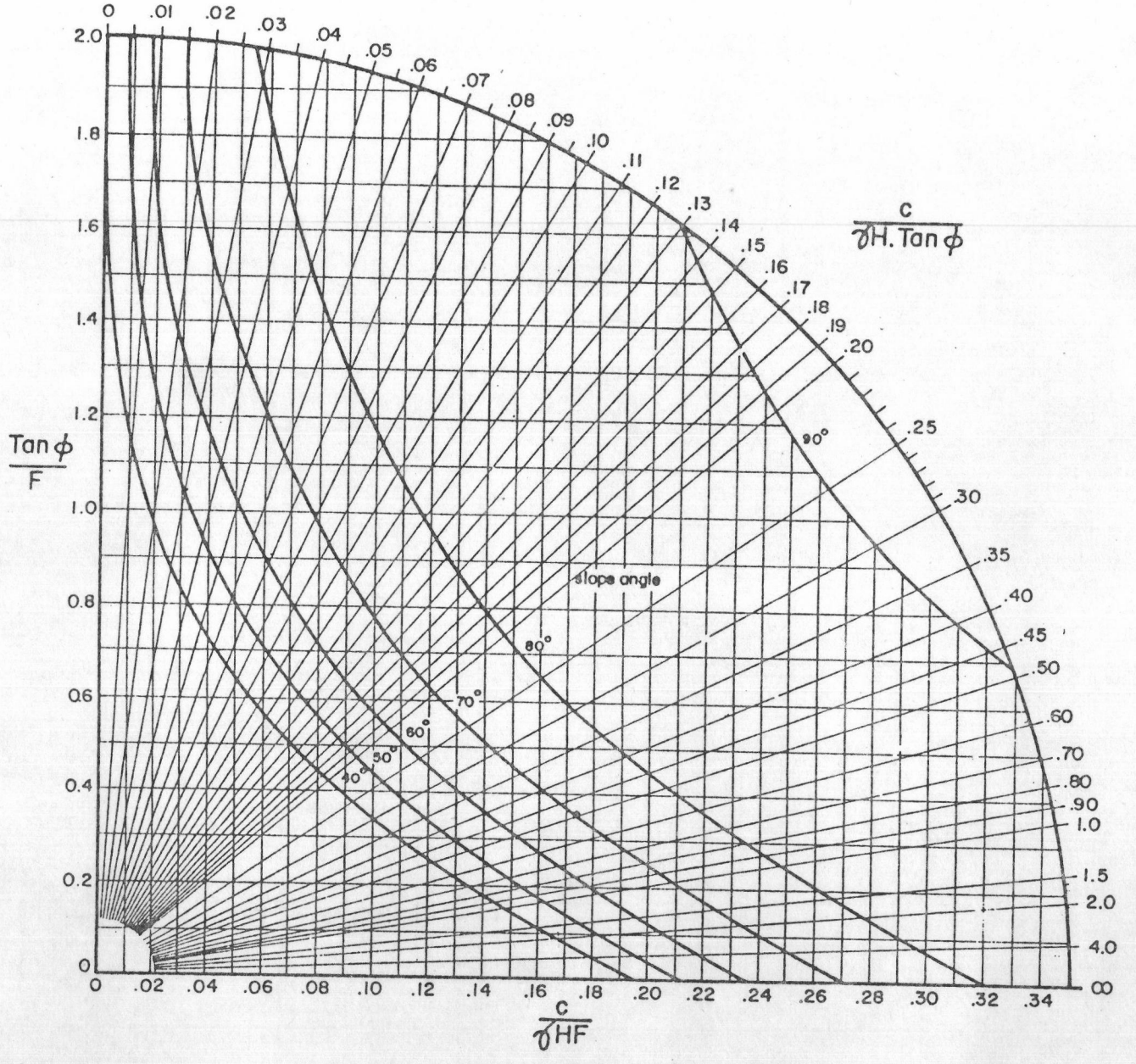

Figure 37. cont.

(d) Circular failure chart number 4.

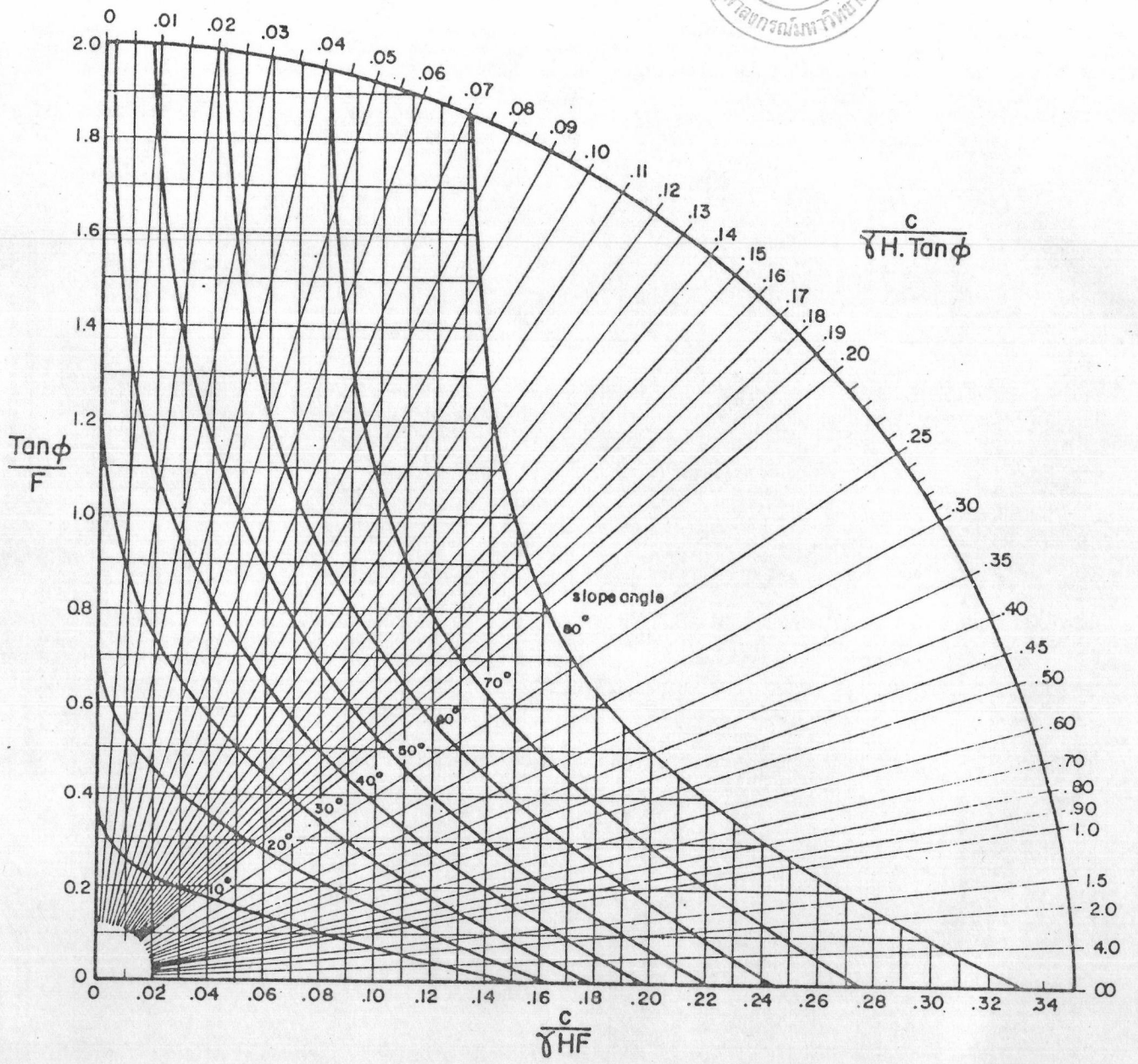

Figure 37. cont.

(e) Circular failure chart number 5.

5.2.2.3 Chose a slope which belongs to the calculated value of $\frac{C}{\gamma H \tan \phi}$

5.2.2.4 Read off either $\tan \phi / F$ (on the ordinate) or $C/\gamma HF$ (on the abscissa) and from this value calculate for the factor of safety, F.

The charts are only approximate and can thus be used as a quick indication of F (or F.S.) of an existing slope or to suggest an appropriate slope angle to be excavated with a required factor of safety.

5.2.3 Simplified Bishop method of slices

In the initial developement of the method of slices for stability analysis (Fellenius, 1936), the side forces on the individual slices were neglected. The factor of safety was satisfied by the equation

$$F = \frac{\Sigma | C_n l_n + (P_n - U_n l_n) \tan \phi_n |}{\Sigma W_n \sin \alpha_n}$$

However, Bishop (1955) proposed another method in which the side forces are taken into the consideration. In this method the mass above the circular-arc failure plane is devided into a resonable number of slices as shown in Figure 38 (a).

Figure 38 (b) shows a typical slice with the side force represented by horizontal component E and vertical component X. The force P_n and thus the strength at the bottom of the slice will different from those where side forces are neglected. The newer method known as Simplified Bishop method of slices is more practically usable . Bishop (1955)

assumed that the forces acting on the sides of any slice have a zero resultant in the vertical direction. Then the factor of safety is given by the equation

$$F = \frac{\Sigma\{|C_n b_n + (W_n - U_n b_n) \tan \phi_n| \frac{\text{Sec } \alpha_n}{1 + (\tan \phi_n + \tan \alpha_n / F)}\}}{\Sigma W_n \sin \alpha_n}$$

where :

C_n = Cohesion of each slices

ϕ = Friction angle of each slices

b_n = Slice width

U_n = Pore pressure which is estimated from phreatic water surface or from equation $U = r_u \gamma h$; r_u = pore pressure ratio, γ = bulk density of slope meterials and h = slice height.

W_n = Weight of each slice = bh

α_n = Angle between the vertical central line of each slice and the radial trace of the failure arc.

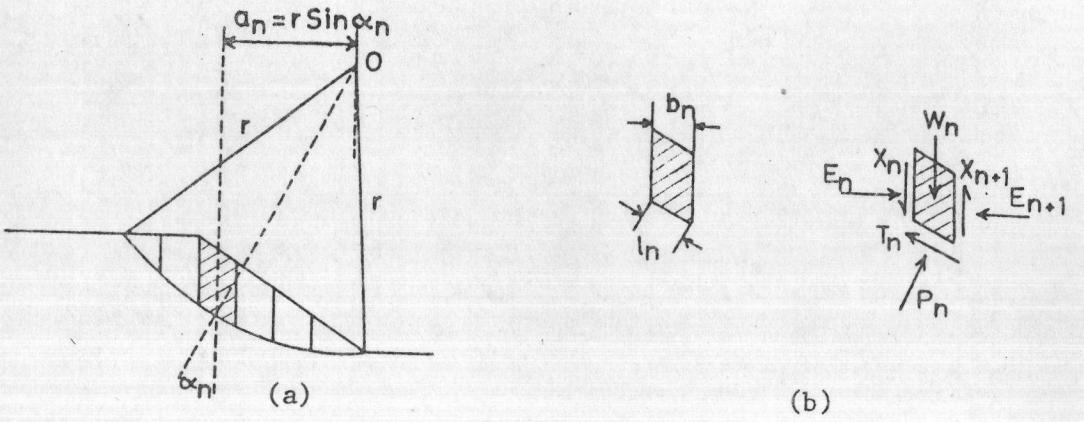

Figure 38. Bishop's method of slices.

5.2.4 Plane failure analysis

Price (1979) proposed the limiting equilibrium equation for plane failure analysis for the situation described in Figure 39

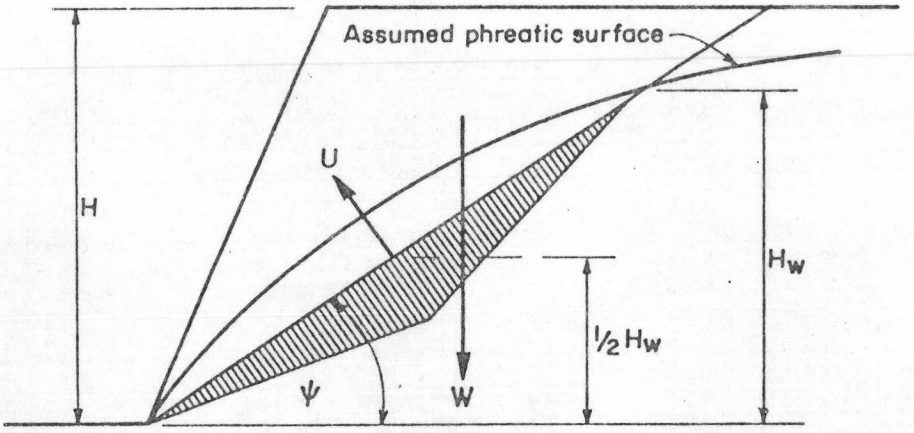

Figure 39. Plane-failure slope with groundwater table.
(after Price, 1979).

For the situation described above, the limiting equilibrium equation (factor of safety = 1) was given by

$$W \sin \psi = c.A + (W \cos \psi - U) \tan \phi$$

where :

$$U = \tfrac{1}{4} \gamma_w H_w^2 \operatorname{cosec} \psi$$

and $$U = \tfrac{1}{4} \gamma_w H^2 \operatorname{cosec} \psi$$, in fully saturated case.

The method of plane failure analysis is especially for Subarea 5 in where the bedding-plane failure dominated.

5.3 Results of Slope Stability Analyses and Discussion

The results of slope stability analyses will be expressed, method by method, as following.

5.3.1 Results from stereographical method

From the stereonet plot according to Markland's technique (Plate 2) of the data observed in the present work, it can be seen that the intersection line of two discontinuities planes falls in the unstable zone, hence gives rise to a wedge failure; and so does the bedding plane which will similarly give rise to a plane failure. Those planes of weakness together with their sliding direction on the unstable slope are illustrated in Table 15.

A Further analysis was done using Hendron et al.'s (1971) technique to find the factor of safety of slope. Poles of those planes of weakness represent potential failure planes indicated by Markland's technique were plotted in an equal-angle stereonet together with their friction cone shown in Plate 2. The factor of safety were calculated and the results are also shown in Table 15. The calculated results indicate that the factor of safety of Subareas 2, 3 and 5 is generally less than unity, thus indicate the unstable condition in these subareas. The calculated results very well agree with the field observation by which the existing of those planes of weakness was noted. As a contrary, other subareas are considerably stable.

5.3.2 Results from Hoek and Bray stability charts method

Circular failure charts numbers 1, 3 and 5 represent the groundwater condition of dry, partially saturated and fully saturated slope respectively. The calculation was carried out for a single-bench slope, two-bench slope, and overall slope of Subareas 1 to 4 respectively.

Table 15. Results of slope stability analyses using the stereographical method.

Subarea	Slope angle		RESULTS OF SLOPE STABILITY ANALYSES				Adjustment of slope angle and comments
			Markland's technique		Hendron et al.'s technique		
	Overall	Individual bench	Stability condition and sliding direction	Plane of weakness caused unstable	$F.S._{max.}$ at $\phi = 22°$	$F.S._{min.}$ at $\phi = 16°$	
1	16°	26°	Stable	Non			No need
2	35°	50°	Unstable N 88°E/50°	J_1 and J_2	0.93	0.63	Decrease 2-4° for individual bench slope.
3	33°	50°	Unstable S 72°E/37° S 71°E/45°	J_2 and F_1 J_2 and F_2	0.67 0.79	0.47 0.56	Decrease 5-10° is possible for individual bench slope.
4	38°	55°	Unstable S 24°E/38°	F_1 and F_2	1.89	1.33	Stability condition due to F_1 and F_2 is considered to be stable.
5	24°	40°	Unstable N 70°W/20-25°	B_5	1.11	0.79	Decrease the slope angle is not possible in the working area.

An example of calculation is shown in Appendix II.

Tables 16 and 17 show the results of factor-of-safety calculation using the maximum and minimum shear strength parameters respectively. It can be seen that the factor-of-safety value of fully-saturated condition is the lowest while that of the partially-saturated condition is in the intermediate, and of the dry condition the highest. This means that the chance of slope failure will be higher during a wet season than during a dry season.

At the maximum shear strength parameters (see Table 16), the factor of safety of overall slope are lower than 1.5 especially in the partially-and fully saturated conditions while the single-bench and two-bench slopes have a comparatively high factor value.

When the minimum shear strength parameters are being considered (see Table 17), the factor of safety of overall slope are slightly larger than the limiting equilibrium (F.S. = 1) in the dry condition, and are lower than unity in partially-and fully saturated conditions. The factor of safety of two-bench slope are slightly larger than unity in partially-and fully saturated conditions while those of single-bench slope are mostly high (F.S. greater than 1.5).

From the reason mentioned above, it shows that the overall slope plays an important role on the slope stability. The chance of slope failure occurred on the overall slope is comparatively higher than the smaller-scale slopes. Therefore, the stability of the overall slope must be considered with a very good care especially when the slope was

Table 16. Results of stability analysis using Circular failure charts method for maximum C, Ø values.

Subarea	Cross-section	Slope	Average factor of safety for Dry slope	Partially sat.	Fully sat.
1	a	1	8.15	6.69	6.32
		2	2.72	-	1.84
		3	2.65	-	1.82
2	a	1	2.79	2.63	2.43
		2	2.08	1.80	1.66
		3	1.87	1.40	1.34
	b	1	3.10	2.96	2.65
		2	2.04	1.83	1.66
		3	1.28	1.20	1.11
3	a	1	3.83	3.51	3.30
		2	2.64	2.21	2.06
		3	1.71	1.27	1.15
	b	1	2.19	2.05	1.84
		2	2.13	1.84	1.68
		3	1.72	1.38	1.26
4	a	1	3.05	2.92	2.69
		2	3.73	2.92	2.73
		3	1.87	1.42	1.35
	b	1	3.77	3.60	3.37
		2	2.14	1.91	1.72
		3	1.44	1.15	1.03

Notations:- Slope 1 = Single bench slope., 2 = Two bench slope.,
3 = Overall slope.

Table 17. Results of slope stability analysis by using Circular failure charts method for minimum C, Ø values.

Subarea	Cross-section	Slope	Average factor of safety for Dry slope	Partially sat.	Fully sat.
1	a	1	4.70	3.91	3.72
		2	1.77	-	1.21
		3	1.23	-	1.19
2	a	1	1.68	1.55	1.43
		2	1.28	1.08	1.00
		3	1.22	0.93	0.60
	b	1	1.83	1.72	1.60
		2	1.25	1.08	0.99
		3	1.03	0.76	0.46
3	a	1	2.31	2.08	1.92
		2	1.60	1.32	1.23
		3	1.02	0.79	0.72
	b	1	1.30	1.21	1.09
		2	1.30	1.10	1.01
		3	1.04	0.81	0.74
4	a	1	1.78	1.68	1.57
		2	2.11	1.73	1.62
		3	1.18	0.89	0.83
	b	1	2.23	2.09	1.87
		2	1.32	1.15	1.04
		3	0.91	0.71	0.63

Notations:- Slope 1 = Single bench slope., 2 = Two bench slope., 3 = Overall slope.

partially- to fully saturated.

5.3.3 Results of simplified Bishop method of slices

Simplified Bishop method of slices was applied to calculate the factor of safety of the overall slope in the partially- to fully saturated condition by differing the pore pressure ratio (r_u) acted on the slip surface of each slice.

The slope height, slope angle, and the value of internal friction angle are used for locating the center of critical failure surface and critical tension crack of each slope profile in case of groundwater present which concordant to the circular failure chart number 3 (see Appendix III). The slope profiles of Subareas 2 to 4, with their failure surfaces, are presented in Plate 4. In the case of Subarea 1, the slope angle is less than 20° and the charts mentioned above are inapplicable for locating the critical failure surface and critical tension crack. This hence suggests that Subarea 1 is more stable than the other subareas.

The parameters used to calculate the factor of safety in each slope profile of Subareas 2 to 4 are only for the cases of partially- to fully saturation. The dry condition is omitted because it is a condition of high stability (see section 5.3.2). It should be noted here that, in the fully saturated condition, the height of water (h_w) is equal to the height of rock mass in each slice (h), thus pore pressure ratio, r_u

$$\text{where } r_u = U/\gamma h \text{ or } \gamma_w h_w/\gamma h,$$

is changed into $r_u = \gamma_w/\gamma$. Substitute the bulk rock density, γ by 2.05 metric ton/m^3 and γ_w by 1 metric ton/m^3, thence $r_u = 0.49$.

For the partially saturated condition r_u was assumed at a rate of 20 %, 50 %, and 70 % of that in fully saturated condition.

The results of calculation are shown in Table 18 while an example of calculation is presented in Appendix III. The results indicate that the factor of safety of Subareas 2, 3, and 4 are generally unstable with the value less than 1.5, or even lower than unity, in partially saturated condition at the value of r_u = 0.24 (50 % saturation), especially when the minimum values of stability parameters are being used. Therefore, the slope of Subareas 2, 3, and 4 are considered as unstable in a long term.

5.3.4 Plane failure analysis of Subarea 5

Three slope profiles consisting of pre-failure slope and failed surface were constructed, as show in Plate 4, to perform back calculation for the required friction angle.

Assuming that the estimated rock blocks in these profiles have a factor of safety of 1.0 at fail, and that there is no cohesion on the failure plane, the required friction angle (ϕ_{req}) can be calculated, using the limiting equilibrium equation mentioned in section 5.2.4, in the cases of dry and fully-saturated slopes respectively. The results of calculation are shown in Table 19 below.

Table 18. Results of slope stability analysis using simplified Bishop method of slices.

Subarea	Cross-section	Groundwater condition	Assume r_u	Factor of safety (F.S.) $F.S._{max}$	$F.S._{min}$
2	a	Partially	0.10	1.86	1.21
		sat.	0.24	1.70	1.09
		"	0.34	1.54	0.95
		Fully sat.	0.49	1.26	0.79
	b	Partially	0.10	1.65	1.06
		sat.	0.24	1.50	0.96
		"	0.34	1.30	0.82
		Fully sat.	0.49	1.09	0.67
3	a	Partially	0.10	1.67	1.07
		sat.	0.24	1.53	0.98
		"	0.34	1.33	0.83
		Fully sat.	0.49	1.13	0.70
	b	Partially	0.10	1.86	1.30
		sat.	0.24	1.71	1.05
		"	0.34	1.50	0.91
		Fully sat.	0.49	1.28	0.75
4	a	Partially	0.10	1.90	1.20
		sat.	0.24	1.75	1.10
		"	0.34	1.55	0.89
		Fully sat.	0.49	1.34	0.81
	b	Partially	0.10	1.49	0.95
		sat.	0.24	1.36	0.85
		"	0.34	1.17	0.73
		Fully sat.	0.49	0.98	0.60

Table 19. Results of back analysis of Subarea 5.

Section	Bench	ϕ_{req} For dry slope (c = 0, U = 0)	ϕ_{req} For fully saturated slope (c = 0, U = ¼ $\gamma_w H^2$ cosec ψ)
a	lower	21	53
b	upper	18	31
	lower	23	47
c	lower	25	46

The results above indicate that the required friction angles in the fully saturated condition are much higher than those in the dry condition. Furthermore, comparing the resultant ϕ_{req} of fully saturated condition with the maximum and minimum available friction angle (ϕ = 22° and 16°) obtained from laboratory test, the latter is generally small. This means that an available friction angle of claystone (ϕ = 16°) is not enough to resist the planar-bedding plane sliding of the blocks.

The factor of safety with respect to friction angle can be calculated. It is defined as the ratio tan ϕ to tan ϕ_{req}. The results of calculation are shown in Table 20.

Table 20. Results of the factor of safety calculation with respect to friction angle.

Section	Bench	Dry slope F.S. 1 (ϕ = 16)	Dry slope F.S. 2 (ϕ = 22)	Fully saturated slope F.S. 3 (ϕ = 16)	Fully saturated slope F.S. 4 (ϕ = 22)
a	lower	0.76	1.05	0.30	0.41
b	upper	0.89	1.22	0.51	0.70
	lower	0.68	0.94	0.34	0.47
c	lower	0.64	0.88	0.35	0.48

From the above results, it clearly indicates that the factor of safety are generally less than unity in both dry and fully-saturated condition. In the other word, the available friction angles of claystones are less than the required friction angle obtained from back calculation, especially in the fully saturated condition. Therefore, the planar sliding are likely to occur in this area where the slope angle is greater than the dip angle of the bedding planes, the latters act as the failure planes.